iScience

CellPress
OPEN ACCESS

Article

Temperature and sex shape Zika virus pathogenicity in the adult *Brat*^{cheesehead} brain: A *Drosophila* model for virus-associated neurological diseases

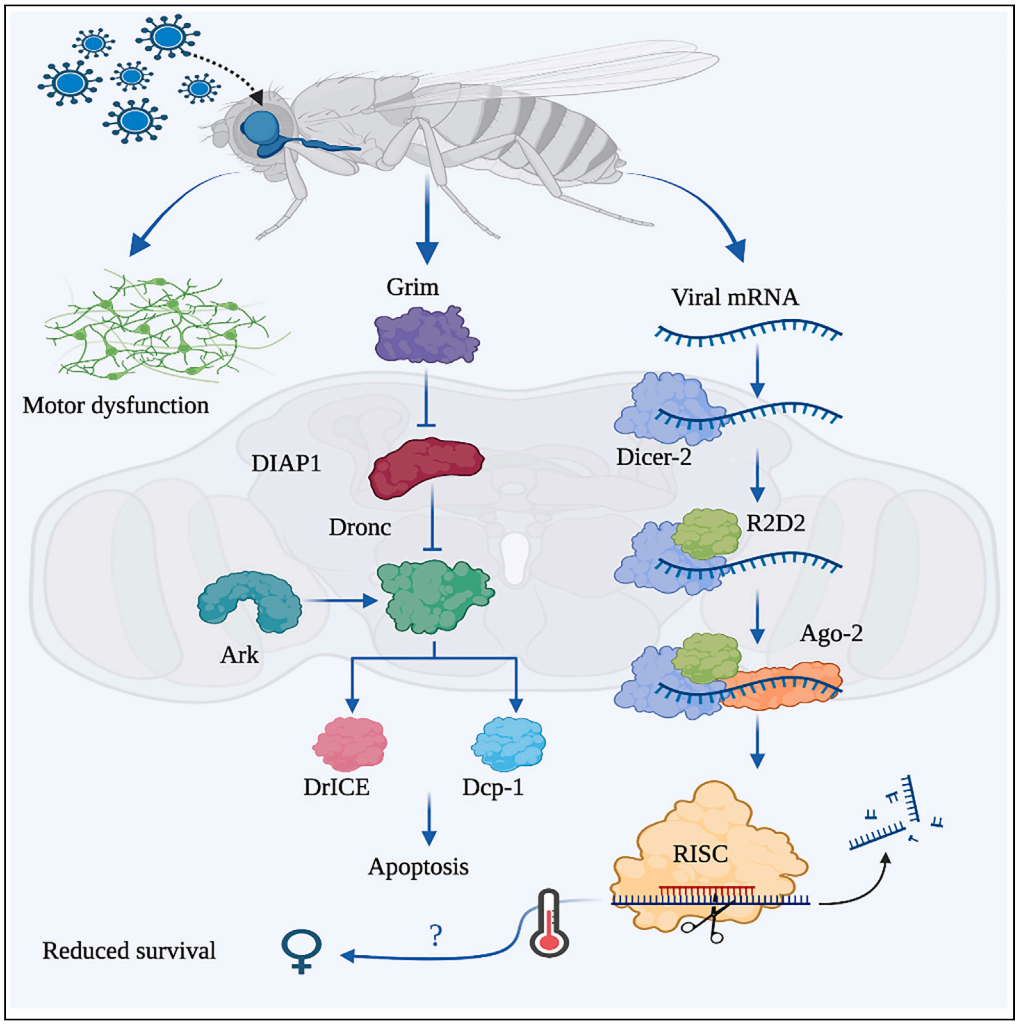

Ghada Tafesh-Edwards, Ananda Kalukin, Dean Bunnell, Stanislava Chtarbanova, Ioannis Eleftherianos

ioannise@gwu.edu

Highlights

Zika virus (ZIKV) replicates at high rates in *Drosophila* adult *brat*^{chs} mutants

ZIKV causes motor dysfunction in a sex- and temperature-dependent manner

ZIKV infection triggers RNAi and apoptosis signaling in the brain of *brat*^{chs} mutants

We establish an *in vivo* model to study virus-associated neurodegenerative disorders

Tafesh-Edwards et al., iScience *26*, 106424
April 21, 2023
https://doi.org/10.1016/j.isci.2023.106424

iScience

CellPress
OPEN ACCESS

Article

Temperature and sex shape Zika virus pathogenicity in the adult *Brat*^{cheesehead} brain: A *Drosophila* model for virus-associated neurological diseases

Ghada Tafesh-Edwards,[1] Ananda Kalukin,[1] Dean Bunnell,[2] Stanislava Chtarbanova,[2,3,4] and Ioannis Eleftherianos[1,5,*]

SUMMARY

Severe neurological complications affecting brain growth and function have been well documented in newborn and adult patients infected by Zika virus (ZIKV), but the underlying mechanisms remain unknown. Here we use a *Drosophila melanogaster* mutant, *cheesehead* (*chs*), with a mutation in the *brain tumor* (*brat*) locus that exhibits both aberrant continued proliferation and progressive neurodegeneration in the adult brain. We report that temperature variability is a key driver of ZIKV pathogenesis, thereby altering host mortality and causing motor dysfunction in a sex-dependent manner. Furthermore, we show that ZIKV is largely localized to the *brat*^{chs} brain and activates the RNAi and apoptotic immune responses. Our findings establish an *in vivo* model to study host innate immune responses and highlight the need of evaluating neurodegenerative deficits as a potential comorbidity in ZIKV-infected adults.

INTRODUCTION

Zika is a single-stranded positive-sense RNA virus that belongs to a mosquito-borne group of flaviviruses such as dengue, yellow fever, Japanese encephalitis, and West Nile. Flaviviruses are mainly transmitted by *Aedes* (subgenus Stegomyia) mosquitoes including *Aedes aegypti* and *Aedes albopictus*.[1] Zika virus (ZIKV) emerged as a global health threat, causing widespread epidemics across the Americas with severe health outcomes in humans.[2] Clinical presentation of ZIKV infection is strongly associated with abnormal functions of neuronal cells causing severe neurological disorders such as microcephaly in newborns and Guillain-Barré syndrome in adults.[3,4] These conditions are characterized by a progressive loss of neuronal tissue and currently remain untreatable. More specifically, research shows that ZIKV directly infects fetal neural stem cells and impairs brain growth, which induces several brain damages including early immature differentiation, apoptosis, and stem cell exhaustion.[5–7] Recent reports of ZIKV active circulation and rising infection cases in densely populated areas of South Asia highlight the high risk of its full-scale resurgence and stress the urgency of understanding host-pathogen interactions and development of targeted treatments and control measures.[8,9]

Drosophila melanogaster has been instrumental in deciphering the molecular mechanisms underlying innate immunity, primarily due to its resourcefulness and abundance of genetic tools. Our current knowledge of immunity in insects is largely owed to the fly model, with some significant genomic and functional approaches uncovering evolutionarily conserved immune mechanisms such as the stimulator of interferon genes (STING) and Toll pathway.[10–13] Moreover, *Drosophila* has been useful for the study of arbovirus infections, especially flaviviruses such as Zika, dengue, and West Nile.[14–16] While not a native host, the broad conservation between *Drosophila* and mosquitoes as dipteran insects allows arboviruses to infect flies and provides novel insights into their pathogenesis and host immune function. As in higher organisms, pathogen infections in *Drosophila* initiate an inflammatory response mediated by the NF-κB signaling pathways Toll and immune deficiency (Imd), resulting in the secretion of antimicrobial peptides (AMPs) to defend the host.[17,18] Even though these antibacterial and antifungal effectors have been widely studied, their roles in antiviral immunity remain largely unknown.[19] Other significant humoral and cellular immunity mechanisms such as the activation of JAK/STAT signaling, autophagy, and melanization are similarly unclear in the context of viral infections in *Drosophila*.[14,20]

[1]Infection and Innate Immunity Laboratory, Department of Biological Sciences, The George Washington University, Washington, DC 20052, USA

[2]Department of Biological Sciences, The University of Alabama, Tuscaloosa, AL 35487, USA

[3]Center for Convergent Bioscience & Medicine, University of Alabama, Tuscaloosa, AL 35487, USA

[4]Alabama Life Research Institute, University of Alabama, Tuscaloosa, AL 35487, USA

[5]Lead contact

*Correspondence: ioannise@gwu.edu

https://doi.org/10.1016/j.isci.2023.106424

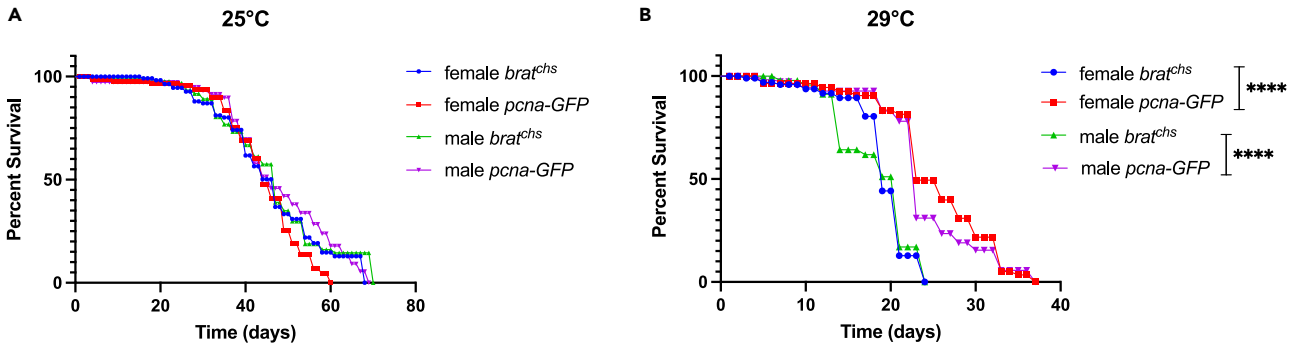

Figure 1. Lifespan assessment of *Drosophila melanogaster* $brat^{chs}$ mutant adult flies and *pcna-GFP* controls

(A) Time course of uninfected female and male flies at 25°C, with mean shown for n = 3.

(B) Time course of uninfected female and male flies at 29°C, with mean shown for n = 3 (****p < 0.0001, log rank test).

Recent studies in *Drosophila* indicate that ZIKV is largely restricted to the brain, where antiviral autophagy is activated to control neuronal infection.[11,21,22] However, the specific molecular innate immune mechanisms that protect neurons against ZIKV infection are unclear. Like humans, neurological disorders and abnormalities in flies can be a result of mutations that affect cell division, as demonstrated with the *Drosophila* mutant *cheesehead* (*chs*) that exhibits both aberrant continued the proliferation of cells and progressive neurodegeneration in the adult brain.[23,24] The name "cheesehead" suitably refers to the numerous holes present in the *Drosophila* brain neuropil. *chs* is an allele of *brain tumor* (*brat*) ($brat^{chs}$), a *Drosophila* gene that has been investigated extensively for its role in asymmetric cell division of neural stem cells (neuroblasts), which limits stem cell proliferation in developing brains.[25–27] *brat* encodes a conserved Tripartite Motif- NCL-1/HT2A/LIN-41 (TRIM-NHL) RNA-binding protein composed of two B-Boxes (zinc finger domains), a coiled-coil domain, which mediates protein-protein interactions, including multimerization, and an NHL domain, which has several functions, including binding to mRNA to regulate translation. Notably, while most reported *brat* alleles have mutations in the NHL domain, the *chs* mutation is in the coiled-coil domain of the TRIM motif.[24,28] The neurodegenerative characteristics of $brat^{chs}$ mutants are intimately linked to neural hypertrophy, a condition that can be relevant to neurodevelopmental and neurodegenerative disorders in humans including ZIKV.[24] Therefore, $brat^{chs}$ mutant phenotype, exhibiting progressive loss of adult brain neuropil in conjunction with massive brain overgrowth, is an ideal model system that allows simultaneous monitoring of ZIKV molecular pathogenesis strategies and host antiviral immune processes in the adult brain.

Interestingly, $brat^{chs}$ mutants are temperature-sensitive for neurodegeneration and survival to eclosion.[24] Early studies show that $brat^{chs}$ mutant flies reared and aged for 2–4 days at 18°C do not show any neurodegeneration, whereas the phenotype was partially penetrant (60% in males and 40% in females) for flies reared and aged for 2–4 days at 25°C and more penetrant (70% in males and 100% in females) for flies reared and aged for 2–4 days at 29°C.[24] The over-proliferation phenotype is also reported to be temperature-sensitive. Brains of $brat^{chs}$ mutant flies reared at 18°C and then shifted to 29°C post-eclosion had no tumors, while $brat^{chs}$ flies reared to adults at 25°C or 29°C do exhibit over-proliferation. However, a significant fraction of $brat^{chs}$ mutants die before eclosion at much more elevated temperatures, such as 29°C.[24] Furthermore, $brat^{chs}$ mutants carrying the *proliferating cell nuclear antigen* (*pcna*)-GFP reporter that labels dividing cells ($brat^{chs}$; *pcna-GFP*), and that were reared at 25°C, were shown to exhibit more severe neurodegeneration and cell proliferation phenotypes than $brat^{chs}$ flies lacking the reporter.[24] Based on this knowledge, our study observes sex and temperature differences to establish how the $brat^{chs}$ mutation contributes to ZIKV infection in correlation to these two factors. Additionally, studies suggest that ZIKV replication is dependent on temperature changes in the host environment, which further calls for a deeper understanding of the molecular immune responses triggered by these temperature changes.[29]

Here we use $brat^{chs}$ mutants to investigate the tissue-specific responses required to regulate innate defenses against ZIKV, thus providing novel insights into the neurological phenotypes associated with this infectious disease. We show that in comparison to controls, ZIKV replicates at higher rates in adult $brat^{chs}$ mutants and causes motor dysfunction in a sex- and temperature-dependent manner, making it imperative

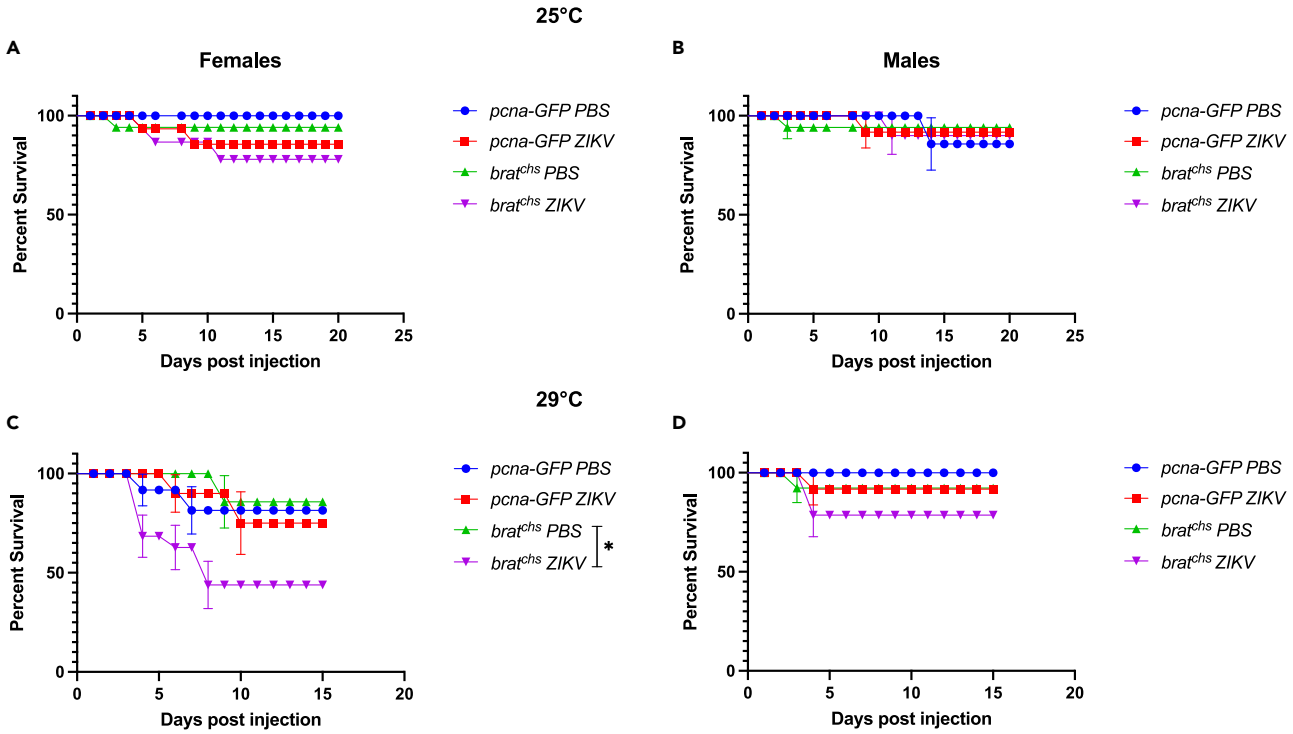

Figure 2. Survival of adult *Drosophila melanogaster* $brat^{chs}$ mutants against Zika virus (ZIKV) varies by sex and temperature

(A–D) Survival of uninfected and ZIKV-infected female and male *brat* mutants and *pcna-GFP* controls at 25°C and 29°C, with mean shown for n = 3 (*p < 0.01, log rank test).

to continue investigating the different responses between female and male flies. We also show that ZIKV infection triggers the RNAi pathway and apoptosis signaling in the brain of $brat^{chs}$ mutants. These important findings add to the very limited literature on ZIKV pathogenesis and the role of RNA-binding proteins such as TRIM-NHL proteins to identify potential therapeutic targets that may prevent or at least minimize the consequences in the early phases of disease and adulthood.

RESULTS

Temperature alters the lifespan of $brat^{chs}$ mutants

Vector-borne flaviviruses including Zika pose a major threat to human health and well-being worldwide. For successful transmission, ZIKV must efficiently enter host cells, propagate within, and survive the extrinsic incubation period (EIP).[30,31] The EIP is an important factor in determining viral transmission potential, as it indicates how long it takes for a vector to become infectious following exposure to the virus. Because this is a temporal process, a vector's lifespan is strongly linked to the EIP and consequently the virus's transmission potential.[31,32] Environmental factors such as temperature influence the aforementioned dynamics of vector-borne disease transmission, as well as vector competence and mortality.[29,33,34] Even though many studies have already documented that the variation in environmental temperature can markedly shape various aspects of virus pathogenicity and vector physiology, the extent to which temperature impacts transmission directly, via effects on pathogen biology, or indirectly, via effects on vector responses to infection, remains largely unknown.[35,36] To this end, we set out to determine how temperature changes influence the lifespan of *brat* mutants, which is relevant for establishing this fly line as a model to study ZIKV and defines any biological constraints on transmission. A time course revealed an average life expectancy of 65 days for both uninfected female and male *brat* mutants at 25°C (Figure 1A) whereas flies maintained at 29°C succumbed at 25 days (Figure 1B). In addition, while female and male *pcna-GFP* flies had a life expectancy similar to their corresponding mutants at 25°C (Figure 1A), the same controls exhibited a shorter lifespan (45 days) at 29°C (Figure 1B). This dramatic decrease across all lines at 29°C indicates a temperature-dependent mortality that will directly impact the ZIKV successful replication and transmission.

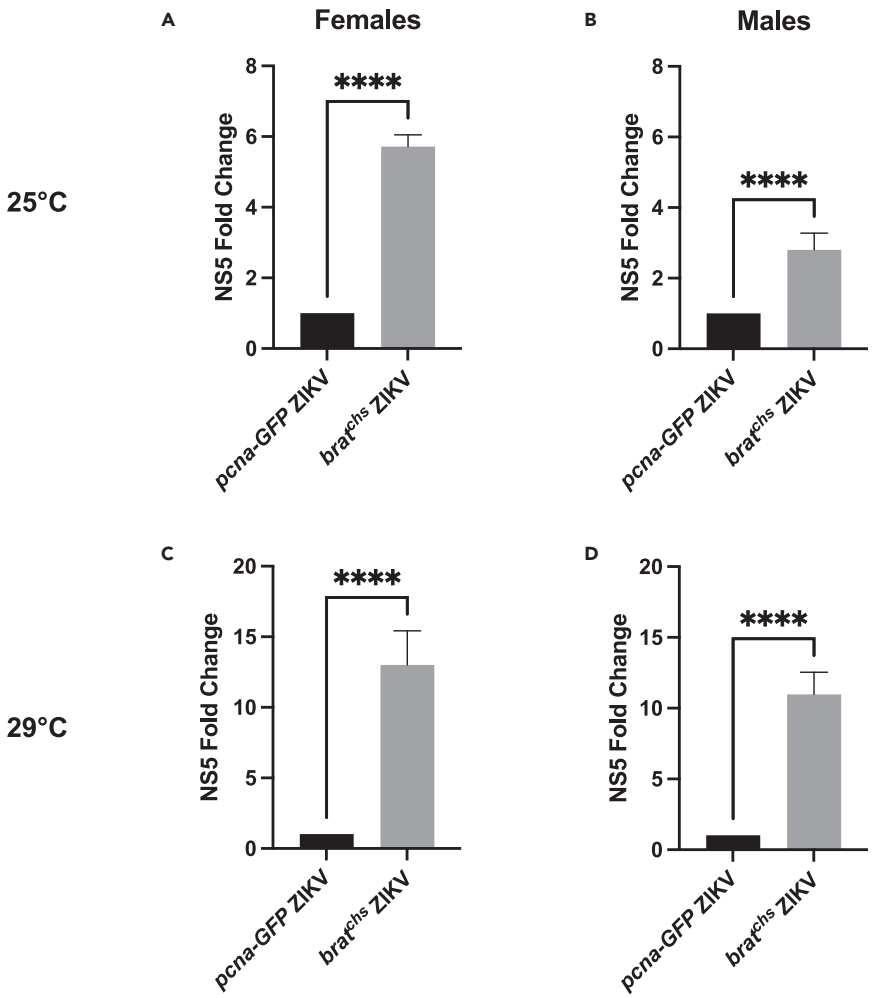

Figure 3. Zika virus (ZIKV) replicates in adult *Drosophila melanogaster brat^{chs}* mutants in a sex- and temperature-dependent manner

(A–D) ZIKV load estimates in female and male *brat* flies at 4 dpi at 25°C and 29°C (fold change to infected *pcna-GFP* controls). Mean ± SEM; n = 3, ****p < 0.0001.

Zika virus replicates in adult *brat^{chs}* mutants in a sex- and temperature-dependent manner

Having established the lifespan of uninfected *brat* mutants, we next determined the flies' survival following ZIKV infection at 25°C and 29°C. We found that the challenge with ZIKV at 25°C failed to reduce fly survivals in *brat^{chs}* females and males, which were similar to the survival rates of PBS- and ZIKV-injected controls (Figures 2A and 2B). Interestingly, survivals of infected *brat^{chs}* females at 29°C were significantly reduced compared to their PBS controls (Figure 2C) whereas infected *brat^{chs}* males at the same temperature showed no significant differences compared to uninfected and infected controls (Figure 2D). We then estimated ZIKV copy numbers in the infected female and male *brat^{chs}* flies at both temperatures compared with their respective *pcna-GFP* controls at 4 days post injection by amplifying *NS5* primer sequences, the largest and most crucial product coded by the ZIKV RNA.[37,38] Both infected female and male *brat^{chs}* mutants showed a significant increase in fold change at 25°C next to infected *pcna-GFP* controls, with female *brat^{chs}* flies exhibiting higher *NS5* levels (3-fold increase) in comparison to males (Figures 3A and 3B). Female and male mutant flies maintained at 29°C showed similar results (Figures 3C and 3D). However, both sexes exhibited strongly elevated ZIKV levels with a doubled fold increase compared to flies kept at 25°C, showing higher ZIKV replication at 29°C. Together, these results show that temperature and sex differences alter ZIKV infection outcomes, thus confirming them as key parameters in disease and immunity studies of this infection.

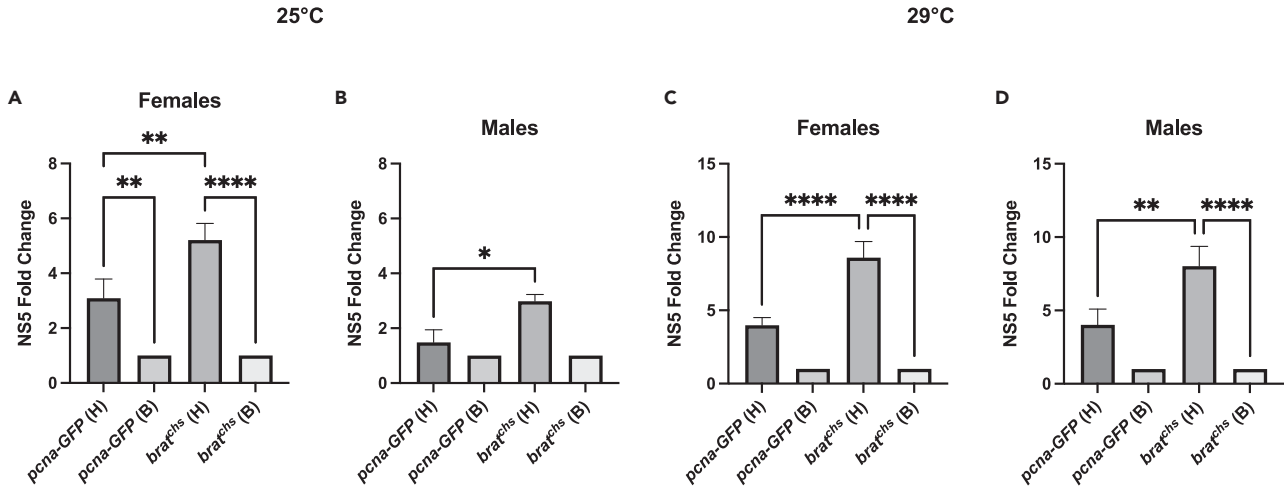

Figure 4. Zika virus (ZIKV) preferentially targets head tissue of adult *Drosophila melanogaster brat^{chs}* mutants at varying rates

(A and C) Female and (B and D) male *pcna-GFP* controls or *brat^{chs}* mutant adult flies were challenged with ZIKV (African strain MR766; 11,000 PFU/fly) and maintained at 25°C or 29°C. Viral load was quantified from heads (H) and bodies (B) by qRT-PCR. Expression levels were normalized to the housekeeping gene *RpL32*, shown relative to bodies of infected flies at 4 dpi with mean ± SEM; n = 3, *p < 0.05, **p < 0.001, ****p < 0.0001.

Zika virus targets the brain of *brat^{chs}* mutants

To further characterize the ZIKV-induced pathology, we systemically challenged *brat^{chs}* mutants and their controls with ZIKV and monitored the infection in the head compared to the body of the flies. *pcna-GFP* flies showed higher *NS5* levels in the heads than bodies, with temperature-dependent replication patterns (Figures 4A–4D) similar to those shown from whole flies at both 25°C and 29°C (Figures 3A–3D). At 25°C, ZIKV load in the heads of female, but not male, *brat^{chs}* flies was substantially higher than the bodies, indicating that ZIKV infects and replicates in the female *brat^{chs}* brain (Figures 4A and 4B). We also observed a significant increase in both female and male *brat^{chs}* brains compared to their controls at 29°C (Figures 4C and 4D). Most importantly, ZIKV copy numbers were strongly elevated in the heads of both female and male *brat^{chs}* mutants compared to their *pcna-GFP* controls at 25°C and 29°C, suggesting that ZIKV directly infects *brat^{chs}* brains and possibly neural stem cells regardless of the temperature changes. To address this possibility, we next sought to determine whether ZIKV antigen co-localizes with cells in the *brat^{chs}* brains that are positive for pcna-GFP. The pcna-GFP reporter transgene is activated in mitotically active cells,[39] and its expression in *brat^{chs}* mutants was reported to mark aberrantly proliferating cells in the adult brain, which are not found in controls.[24] Immunostaining using the anti-flavivirus envelope protein antibody 4G2 revealed the presence of ZIKV in the brains of both *pcna-GFP* controls and *brat^{chs}* mutants (Figure 5). PBS-injected brains did not display marked ZIKV staining (Figure 5A). Consistent with the gene expression analysis, we observed that ZIKV staining was more widespread in the brains of *brat^{chs}* mutants (1.33% stained area) in comparison to *pcna-GFP* controls (1.15% stained area) based on immunofluorescence quantification in Fiji ImageJ2. In PBS-injected controls, the background levels of stained area were 0.94% and 0.93% for both genotypes, respectively (Figure 5B). In *brat^{chs}* mutants we find some co-labeling of GFP-positive cells and ZIKV (Figures 6 and 7); however, the majority of GFP-positive cells are not ZIKV-positive. We found that in both controls and *brat^{chs}* mutants, ZIKV does co-localize with Repo (Reversed-polarity) and with Elav (Embryonic lethal, abnormal vision), which are glial and neuronal cell markers, respectively. Yet, for most of the ZIKV labeling we did not find it to co-localize with the examined markers (Figures 6 and 7). We note; however, that both Repo and Elav target transcription factors with nuclear localization in the cell while the pcna-GFP reporter is not exclusively nuclear.

Zika virus induces severe motor dysfunction in *brat^{chs}* mutants

Drosophila has been widely used as a model system to study neurodegenerative disorders such as Alzheimer's and Parkinson's diseases.[40,41] In particular, locomotion, the major output of the nervous system, is used to identify and study molecules or genes involved in these disorders. Consistently, locomotor impairment is a common phenotype of neurodegeneration that can be characterized in *Drosophila* with simple climbing assays.[42–45] These assays take advantage of *Drosophila*'s natural tendency to climb upward against gravity, a robust and reproducible behavior known as negative geotaxis. They are reliable

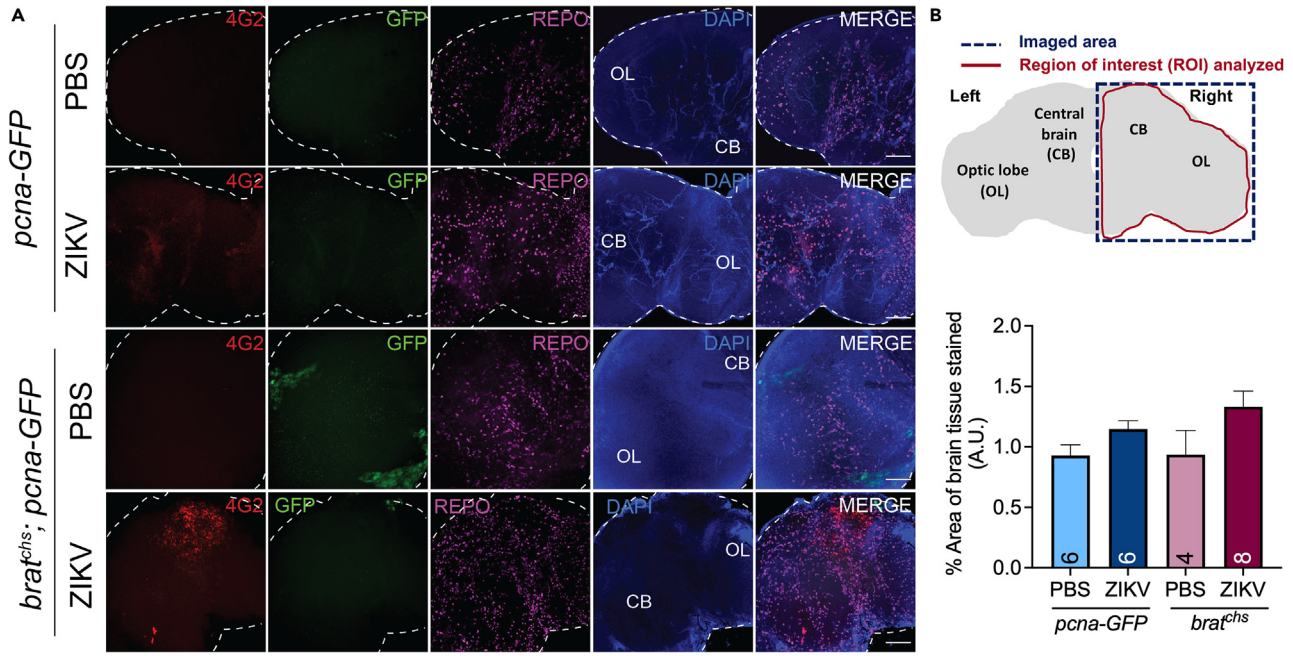

Figure 5. Zika virus (ZIKV) infects the brain of adult *Drosophila melanogaster brat^{chs}* mutants

(A) Female *pcna-GFP* controls or *brat^{chs}; pcna-GFP* mutant adult flies were challenged with ZIKV (African strain MR766; 11,000 PFU/fly) and maintained at 29°C. Immunostaining co-labeling for the ZIKV antigen, GFP (proliferating cells), and Repo (glia) 4 dpi. More widespread 4G2 labeling is observed in brains of *brat^{chs}* flies in comparison to *pcna-GFP* controls. Representative confocal stack images are shown (n = at least 2 analyzed brains containing 4 imaged areas/condition). Scalebar: 50 μm. OL: optic lobe, CB: central brain. (B) Top: Representation of the right brain area imaged (discontinued blue line frame) within which a region of interest (ROI) (area limited with the continuous red line) was selected for quantification with Fiji for each confocal image analyzed. Both left and right sides of each brain were imaged (n = 2 imaged areas/brain). Bottom: Quantification of ZIKV antigen immunostaining in brains of *brat^{chs}* and *pcna-GFP* flies subjected to PBS injection (control) or ZIKV infection (African strain MR766; 11,000 PFU/fly). Bar graphs represent mean ± SEM arbitrary units (A.U.) values of the % stained area in all ROIs analyzed. Quantified n number of imaged areas for each treatment group is shown within respective bars.

parameters that provide a quantitative, cost-effective, general tool for measuring locomotor behaviors of wild-type and mutant flies in detail and can reveal subtle or severe motor defects, which are crucial to understanding the manifestation of locomotor disorders. Because ZIKV is closely associated with neurodegeneration, we performed a climbing assay to determine the behavioral phenotypes triggered by the virus in the *brat^{chs}* mutants. Infected *pcna-GFP* flies showed longer climbing times compared to uninfected controls at both 25°C and 29°C (Figure 8). In addition, we found that the climbing ability and speed were severely affected in infected female *brat* flies at 25°C with only 30% of these flies being able to climb compared to 55% of uninfected controls and %70 of infected controls (Figures 8A and 8B). Infected *brat^{chs}* males kept at 25°C also showed lower climbing ability and speed compared to infected controls (Figures 8C and 8D). In addition, both *brat^{chs}* female and male flies kept at 29°C displayed similar locomotive defects compared to their respective controls, therefore reflecting severe locomotor impairment as a disease outcome (Figures 8E–8H). Collectively, these results suggest that the detection of locomotion defects may contribute to understanding symptomatic behaviors associated with neurodegenerative pathology using the *brat^{chs}* model.

Zika virus infection activates the antiviral RNAi pathway in the brain of *brat^{chs}* mutants

The canonical RNA interference (RNAi) pathway is one of the major evolutionarily conserved defense mechanisms against arboviral infections in insect hosts.[20,46,47] In *Drosophila*, the RNAi pathway is initiated by the enzyme Dicer-2, which acts as a pattern recognition receptor that detects virus-derived double-stranded RNA (dsRNA) and generates small interfering RNAs (siRNAs). These viral siRNAs are subsequently loaded onto an RNAi-induced silencing complex (RISC) with Argonaute-2 (Ago2) as a central molecule. The complex then identifies complementary endogenous sequences, eventually leading to the cleavage and degradation of viral RNA after specific siRNA-mRNA hybridization.[48] To examine whether ZIKV infection stimulates this antiviral response in *brat^{chs}* mutants, we determined the transcript levels of the RNAi machinery Dicer-2 and Ago-2 in infected female and male flies. We found that the

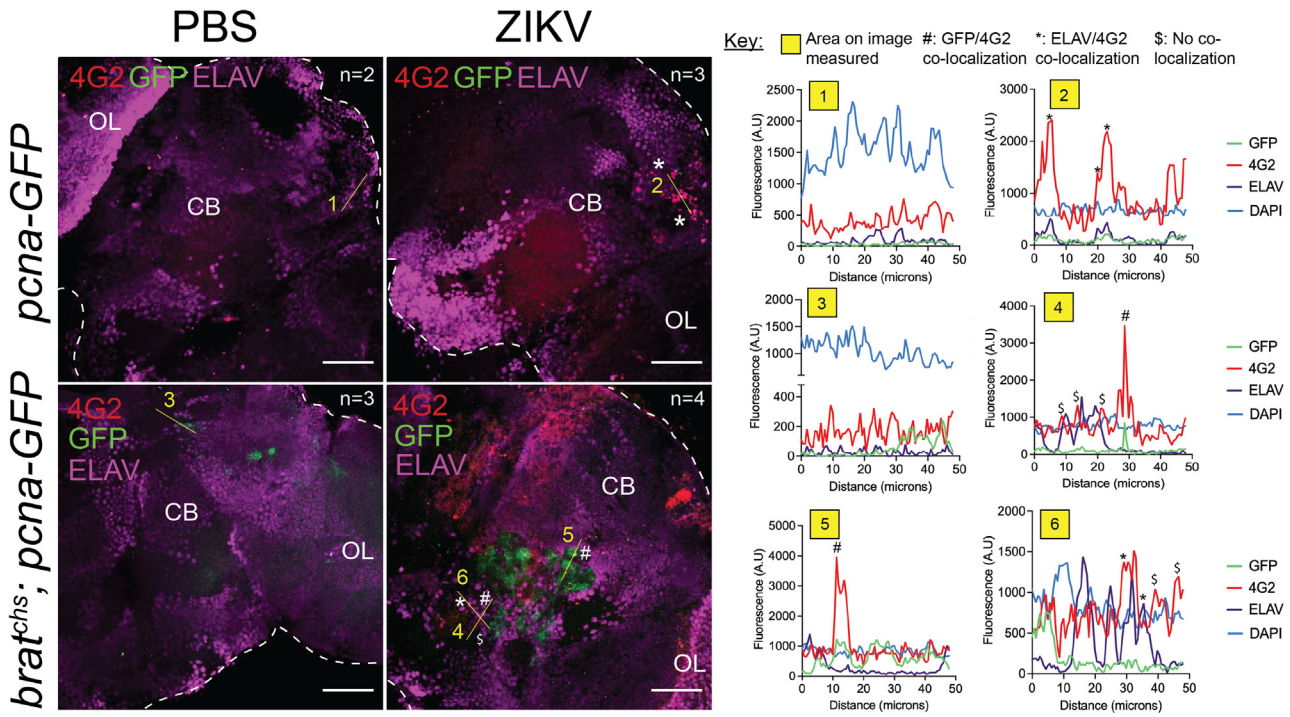

Figure 6. Zika virus (ZIKV) infects neurons and progenitor cells in the brain of adult *Drosophila melanogaster brat^{chs}* mutants

Left panels: male *pcna-GFP* controls or *brat^{chs}; pcna-GFP* mutant adult flies were challenged with ZIKV (African strain MR766; 11,000 PFU/fly) and maintained at 29°C. Immunostaining co-labeling for the ZIKV antigen, GFP (proliferating cells), and Elav (neurons) shows some co-localization between GFP-expressing cells and ZIKV (pound symbol) in mutants, and Elav (asterisks) in both mutants and controls. The $ symbols indicate ZIKV staining that does not co-localize with Elav or GFP. Representative confocal stack images are shown (number of brains analyzed (n)/condition is indicated on the top right part of each respective image). Right panels: Fluorescence intensity plots in selected areas of the brain (yellow lines connecting two points labeled 1–6) for indicated samples. Overlapping peaks within each intensity plot were labeled as co-localizing. Note that DAPI staining is not shown in confocal stack images in the left panels, however it is represented in the intensity plot. Scalebar: 50 μm. OL: optic lobe, CB: central brain, A.U.: arbitrary units.

heads of *brat^{chs}* females kept at both 25°C and 29°C showed significantly upregulated Dicer-2 and Ago-2 expression levels compared to their bodies, consistent with our findings that ZIKV targets the brain (Figures 9A and 9C). This effect was also observed in *brat^{chs}* female heads compared to the *pcna-GFP* heads, indicating that the virus and the *brain tumor* gene mutation possibly enhance the host immune response (Figures 9A and 9C). In contrast, *brat^{chs}* male heads showed only significantly higher Ago-2 expression at 25°C compared to their bodies and infected control heads (Figure 9B). This was not the case in infected male mutants kept at 29°C, as only Dicer-2 was significantly elevated in *brat^{chs}* male heads compared to *pcna-GFP* heads, thus further confirming this effect as an outcome of the *brat^{chs}* gene mutation (Figure 9D). Together, these results show that the RNAi pathway is activated against the ZIKV infection in the brain in a sex-dependent manner with temperature changes only evident in males. Also, ZIKV has a synergistic effect that enhances the host immune response activation against the *brain tumor* mutation and its resulting defects.

Zika virus infection triggers apoptosis in the brain of *brat^{chs}* mutants

ZIKV is known to cause severe congenital and autoimmune neurological complications such as microcephaly in infants and Guillain-Barré syndrome in adults.[49–52] ZIKV infection is especially linked to apoptotic cell death and cell-cycle disruption, providing a plausible mechanism for cellular stress responses and the resulting neurological defects.[53,54] More specifically, ZIKV has been shown to reduce neural progenitor cell proliferation, induce their premature differentiation, and activate apoptosis to target them along with immature neurons.[54,55] Given this, the neural over-proliferation and neurodegeneration caused by the *brat^{chs}* mutation in the adult *Drosophila* brain provide an excellent model to investigate the mechanisms underlying both conditions and possibly develop therapeutic strategies and more targeted treatments for ZIKV neurologic disorders. To test whether ZIKV challenge activates

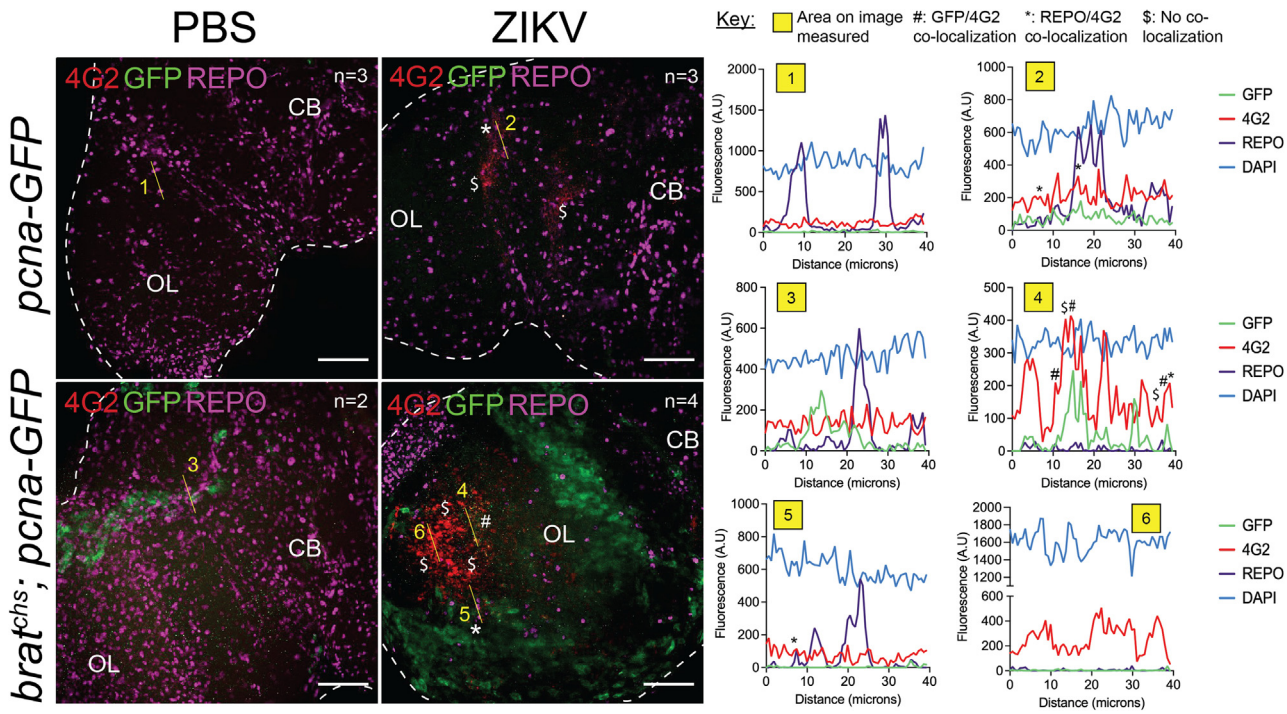

Figure 7. Zika virus (ZIKV) infects glia in the brain of adult *Drosophila melanogaster brat^{chs}* mutants and *pcna-GFP* controls

Left panels: female *pcna-GFP* controls or *brat^{chs}; pcna-GFP* mutant adult flies were challenged with ZIKV (African strain MR766; 11,000 PFU/fly) and maintained at 29°C. Immunostaining co-labeling for the ZIKV antigen, GFP (proliferating cells), and Repo (glia) shows some co-localization between GFP-expressing cells and ZIKV (pound sign) in mutants, and Repo (asterisks) in both mutants and controls. The $ symbols indicate ZIKV staining that doesn't co-localize with Repo or GFP. Representative confocal stack images are shown (number of brains analyzed (n)/condition is indicated on the top right part of each respective image). Right panels: Fluorescence intensity plots in selected areas of the brain (yellow lines connecting two points labeled 1–6) for indicated samples. Overlapping peaks within each intensity plot were labeled as co-localizing. Note that DAPI staining is not shown in confocal stack images in the left panels; however, it is represented in the intensity plot. Scalebar: 50 μm. OL: optic lobe, CB: central brain, A.U.: arbitrary units.

programmed cell death in the *brat^{chs}* brain, we estimated the transcriptional activation levels of the three *Drosophila* pro-apoptotic genes *hid*, *grim*, and *reaper* in the heads and bodies of mutants via RT-qPCR. We found that *grim* expression was significantly increased in the heads of infected *brat* female and male mutants, at both 25°C and 29°C, compared to their bodies and infected controls (Figures 10A–10D). Notably, *grim* was also significantly upregulated in the heads of *pcna-GFP* heads compared to their bodies, confirming that ZIKV infection activates apoptosis in the adult *Drosophila* brain. We observed no significant differences in the expression levels of genes *hid* and *reaper* among any of the various treatment groups and conditions, which highlights a mechanism through which *grim* induces apoptosis in response to ZIKV infection (Figures 10A–10D).

DISCUSSION

Here we examine ZIKV pathogenesis in the presence of *cheesehead*, a mutation of *brain tumor* in *Drosophila*, and establish *brat^{chs}* flies as a tractable experimental system to investigate the effects of ZIKV on the immune signaling and function in the adult *Drosophila* brain. Using this particular *Drosophila* model offers an advantageous insight in the case of neurodegenerative diseases due to *brat*'s role as an RNA-binding protein from the TRIM-NHL family. During the asymmetric division of *Drosophila* neuroblasts, brat localizes at the basal cortex via direct interaction with the scaffolding protein Miranda and segregates into the basal ganglion mother cells after cell division. The *cheesehead* mutation in this model is in the coiled-coil domain, which acts as a scaffold for regulatory protein complexes; not the RNA-binding domain (NHL), which binds to mRNA and other RNA regulatory proteins, including Miranda.[24,56] This in turn represents a previously unknown role for *brat* that could reveal a new pathway that is relevant to human neurodegenerative diseases such as these caused by Zika with a possible implication in immunity against RNA viruses.

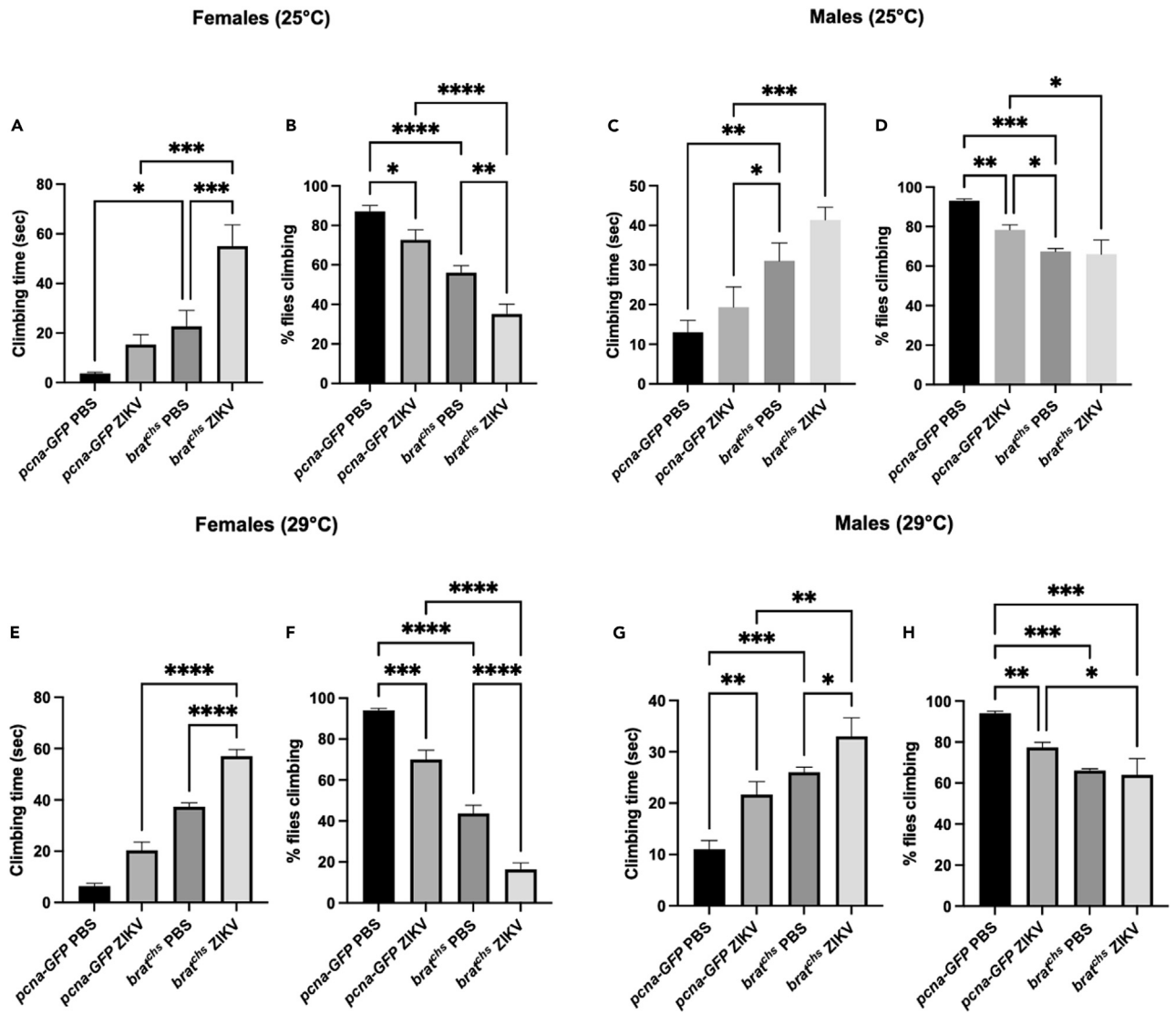

Figure 8. Zika virus (ZIKV) infection significantly impairs motor function in *Drosophila melanogaster* $brat^{chs}$ mutant adult flies

Climbing ability and speed of climbing in uninfected and ZIKV-infected female and male controls and *brat* mutant flies at (A–D) 25°C and (E–H) 29°C, with mean shown for n = 3, *p < 0.01, **p < 0.001, ***p = 0.0001, ****p < 0.0001.

Our findings indicate that higher temperature dramatically alters the longevity, climbing ability, and immunity of $brat^{chs}$ mutants and their *pcna-GFP* controls in both males and females, suggesting a temperature-dependent host fitness that modifies infection outcomes. $brat^{chs}$ mutants are temperature-sensitive for neurodegeneration and over-proliferation in adult brains, providing a unique opportunity for the genetic analysis of *brat* function that was not feasible before. For instance, this mutation can be a useful tool for the suppression or enhancement of the adult over-proliferation and/or neurodegeneration phenotypes to determine other genes with which *brat* interacts to regulate differentiation and growth. This is particularly crucial during infections such as Zika which inhibit brain development, as it will provide a valuable platform to screen for therapeutic candidates that arrest or block the impact of such diseases on neural development.

Understanding how vectors respond to environmental variations, including temperature, is especially relevant for establishing how vector-borne pathogens emerge and spread, hence defining the biological constraints on vector transmission and competence. In this study, we model the effects of temperature on ZIKV, which belongs to the widespread and important flavivirus family that currently lacks complete temperature-dependent models. Our results show that ZIKV replication in $brat^{chs}$ flies is optimized at 29°C, which

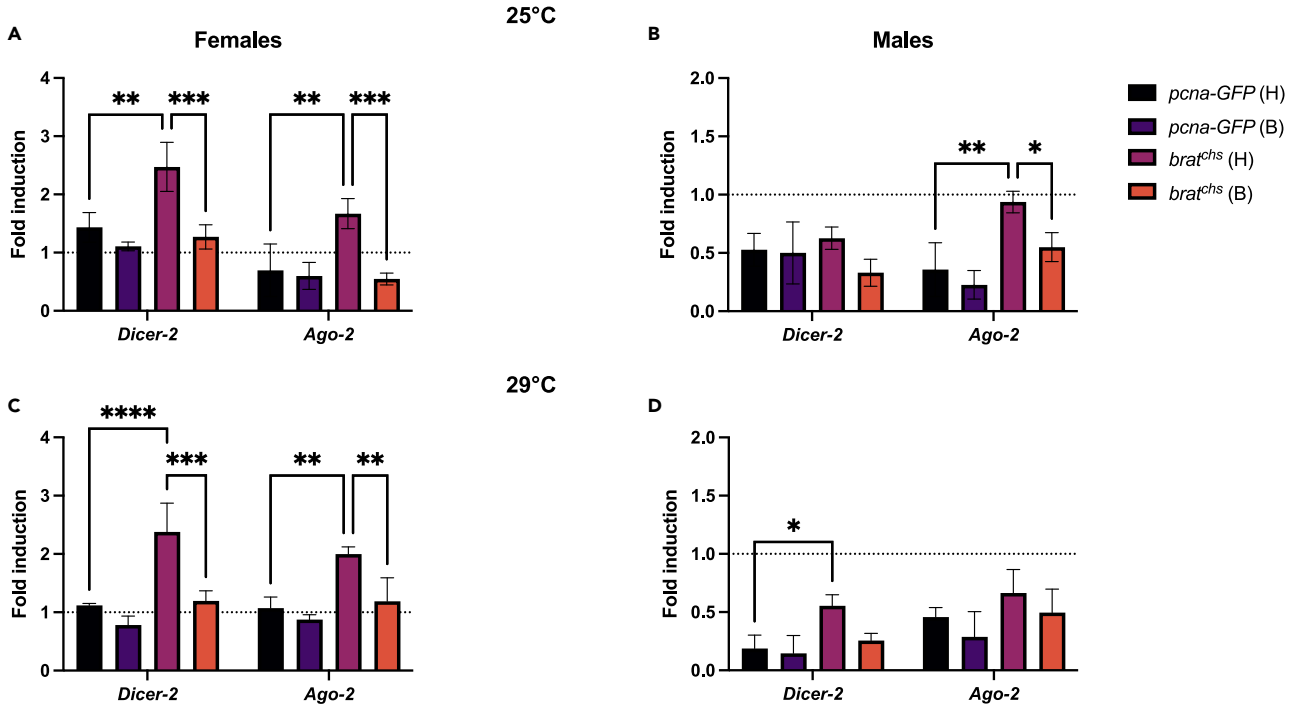

Figure 9. Zika virus (ZIKV) infection triggers the RNAi pathway in the brain of *Drosophila melanogaster* $brat^{chs}$ mutant adult flies

Transcript levels of RNAi machinery, *Dicer-2* and *Ago-2* in heads (H) and bodies (B) of ZIKV-infected female and male $brat^{chs}$ and *pcna-GFP* flies at (A and B) 25°C and (C and D) 29°C. Expression levels are normalized to the housekeeping gene *RpL32* and shown relative to uninfected controls. Mean ± SEM; n = 3, *p < 0.01, **p < 0.001, ***p = 0.0005, ****p < 0.0001.

contributes to significant advances in our knowledge of the physiological and molecular interactions between pathogens and mosquito vectors.[29,33] Temperature variation may alter the ZIKV infection process either through changing the *Drosophila* response to the infection, modifying the efficiencies of viral-specific processes, or, more likely, both. Our study focused on fly responses and ZIKV pathology in the brain early in the infection process. However, disentangling the observed effects will require further analysis of the combinatorial effects of the *cheesehead* mutation and its characteristic phenotypes in the adult brain. Sampling of other immunological tissues and at later time points during which high levels of ZIKV can be detected will also contribute to our understanding of the physiological and molecular interactions between the virus and its host. Nonetheless, while further work is needed to determine the precise mechanisms at play, results from this study indicate that temperature shifts the balance and dynamics of the host environment, which results in direct and indirect consequences for the ZIKV infection process.

Our findings indicate that sex is a significant factor in response to ZIKV infection and its outcome. Even though ZIKV replicates in similar trends in each experimental sex group and its corresponding controls at different temperatures, only female $brat^{chs}$ flies succumbed to the infection at 29°C. Moreover, we detected higher ZIKV levels from whole bodies and heads of infected female $brat^{chs}$ compared to their male counterparts. Infected female $brat^{chs}$ also exhibited more severe motor dysfunction and elevated immune responses compared to $brat^{chs}$ males, thus suggesting that sex differences in immune responses result in the differential susceptibility of females and males to ZIKV infection (Figure 11). Such dimorphic survival and pathology could result from inherent costs associated with the induction of enhanced immune responses, whereby female mutants that raise a more potent immune response against ZIKV induce greater tissue damage that leads to higher mortality at 29°C. Similar immune studies investigating bacterial, viral, and fungal infections have also presented evidence of sexual dimorphism and sexual antagonism for resistance and tolerance, and a trade-off between the two traits.[57–59] However, the mechanisms underpinning these findings are largely unresolved due to a lack of information about sex-specific genetic regulation of molecular immunity in *Drosophila*. While there is a growing interest in studies exploring antiviral immunity and in reporting both sexes, most work in this field uses only one sex or does not stratify by sex.[57,60] We recently reported sexually dimorphic responses to ZIKV infection, which is consistent with the evidence presented here.[61] Therefore, sex is an essential factor that impacts immunity and must be

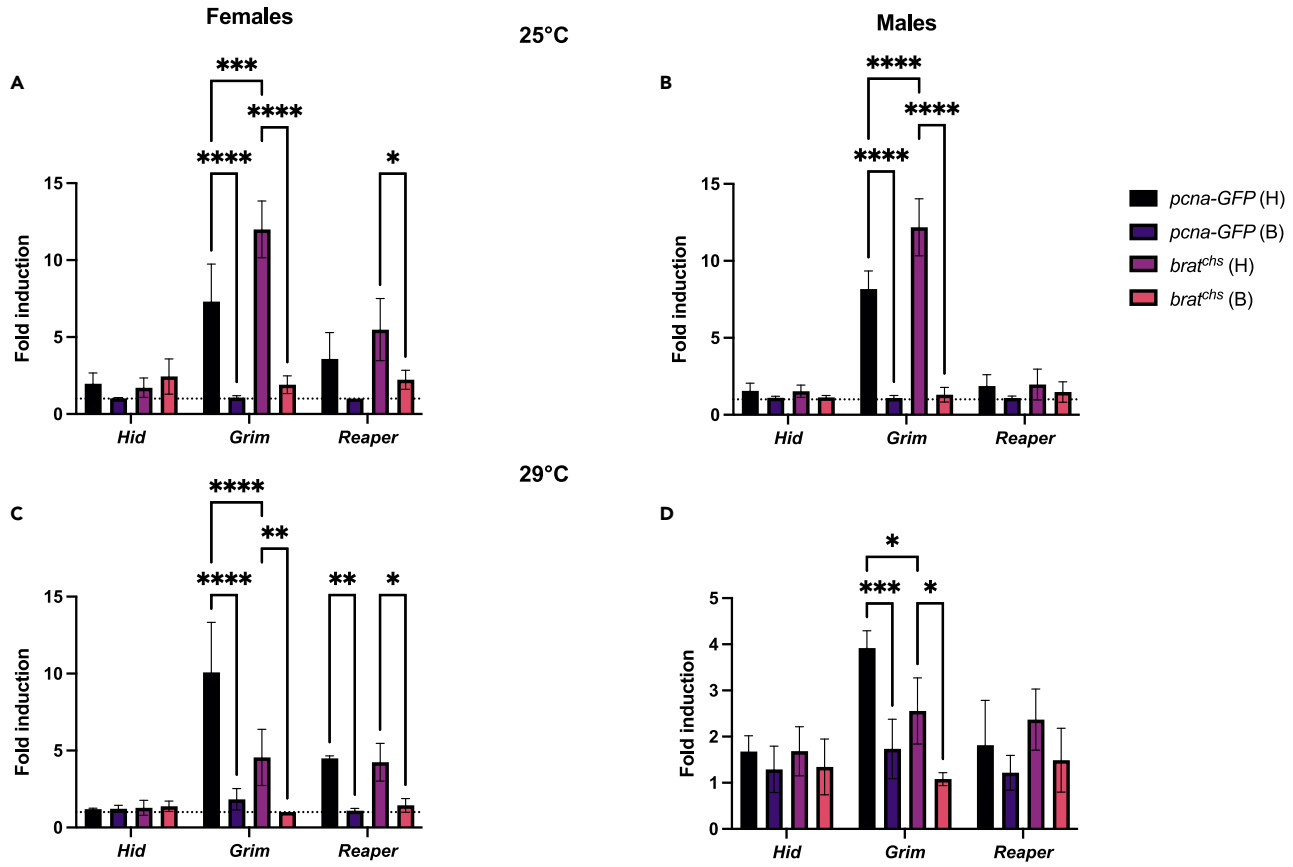

Figure 10. Zika virus (ZIKV) infection activates apoptosis in the brain of *Drosophila melanogaster brat^{chs}* mutant adult flies

Quantitative RT-PCR analysis of *pcna-GFP* controls and *brat^{chs}* heads (H) and bodies (B) was performed to quantify apoptotic *Hid*, *Grim*, and *Reaper* gene expression at (A and B) 25°C and (C and D) 29°C. Expression levels are normalized to the housekeeping gene *RpL32* and shown relative to uninfected controls. Mean ± SEM; n = 3, **p < 0.05, **p < 0.001, ***p = 0.0007, ****p < 0.0001.

considered in the interpretation of data arising from similar immunological studies to improve rigor and reproducibility. These sex differences can potentially be exploited to gain valuable insight into the mechanistic underpinnings of hormonal, genetic, and environmental effects on infectious diseases, as well as the outcome of potential vaccinations for various individuals.

This research contributes to advances in the characterization of ZIKV-induced pathology in *Drosophila* by investigating the molecular events leading to the activation of immune responses. Consistent with previous studies,[11] we report that ZIKV is preferentially localized in the heads of female and male *brat^{chs}* flies, as well as in respective *pcna-GFP* controls. The immunostaining co-labeling for the ZIKV antigen, GFP (proliferating cells), Repo (glia), and Elav (neurons) detected some ZIKV/GFP co-localization in *brat^{ch}* brains and some ZIKV/Elav and ZIKV/Repo co-localization in both controls and mutants. Interestingly, however, the majority of ZIKV staining did not co-localize with the examined markers. This indicates that it is likely that some progenitor cells that are among proliferating cells in *brat^{chs}* mutants[24] are infected, as well as that both neurons and glia are targeted by the virus in the adult *Drosophila* brain. However, because both Repo and Elav are transcription factors with nuclear localization in differentiated cells, we cannot exclude the possibility that ZIKV targets neurons and glia more widely in the adult brain. The antibodies we used label transcription factors in the nucleus without staining the cytoplasm and therefore further experiments are warranted to fully define the exact cell types targeted by ZIKV in the adult *Drosophila* brain and in *brat^{chs}* mutants. For instance, one future experiment to consider is to generate fly lines that label each cell type with a cytoplasmic or membrane-targeted red fluorescent protein (RFP) and co-stain for ZIKV and anti-RFP. Furthermore, it is possible that we are also not capturing the exact neural progenitor stage (e.g., neuroblast, intermediate neural progenitor, ganglion mother cell, and so forth) targeted by

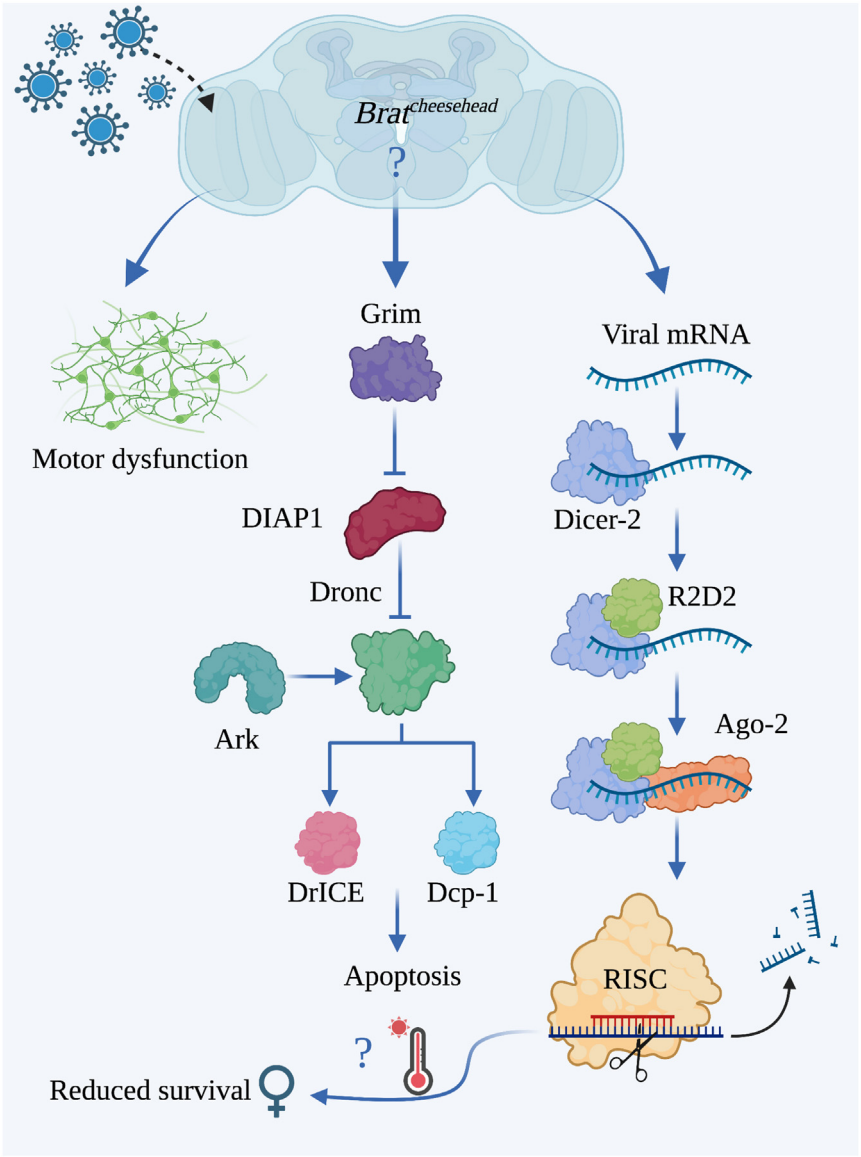

Figure 11. Model for Zika virus (ZIKV)-induced responses in the *Drosophila melanogaster brat^{chs}* mutant adult flies

In addition to causing climbing defects, ZIKV infection activates the RNAi and apoptosis signaling pathways in the brains of female and male *brat^{chs}* mutant adult flies. RNAi is the main antiviral immune response that activates Dicer-2 and Ago-2 as the central operating genes driving sequence-specific degradation of viral RNA. Apoptosis, on the other hand, requires the transcriptional activation of *Grim* which binds to and antagonizes *Drosophila* inhibitor of apoptosis proteins (DIAPs) to inhibit caspases. Despite the presence of higher ZIKV loads and the upregulation of these immune pathways in both sexes, only female *brat^{chs}* mutant flies die faster than infected and uninfected controls at higher temperatures, indicating temperature effects and other possible, yet unknown, viral mechanisms that overcome the female fly immune responses. Future studies can utilize this *brat^{chs}* model to further dissect the molecular and pathophysiological basis of host-ZIKV dynamics.

ZIKV by only using the pcna-GFP reporter. Refining the cell types targeted by ZIKV could also help map the behavioral changes resulting from ZIKV infection such as impaired climbing, thus providing further insights into the underlying pathophysiological mechanisms.

By developing an *in vivo* model for studying the molecular basis of innate immunity against ZIKV infection, we also show that the main mediators in the RNAi antiviral response, Dicer-2 and Ago-2 are upregulated in

the context of ZIKV infection in the *Drosophila* brain. How exactly these RNAi effectors regulate viral replication in the brain and whether the differential roles we observed in the two sexes affect host-ZIKV interactions remain largely unclear. In a recent report, Dicer-2 was implicated as instrumental in regulating ZIKV replication while Ago-2 was dispensable.[62] This distinction in the level of surveillance between the two RNAi components is likely due to the involvement of Dicer-2 in other immune pathways such as Toll signaling and expression of the antiviral gene *Vago*.[63,64] Identification of putative ZIKV dsRNA targets recognized by Dicer-2 may provide more insight into its intricate function during ZIKV and other flavivirus infections in *Drosophila*. Consistent with our findings that ZIKV targets the $brat^{chs}$ brain, we, for the first time, also show that the *Drosophila* apoptotic gene *Grim* is associated with increased activation of the antiviral RNAi pathway in response to ZIKV infection in the adult brain. Notably, at 25°C *Grim* expression in the $brat^{chs}$ flies was higher than that of *pcna-GFP* controls and vice versa at 29°C. This finding can be attributed to the hypomorphic nature of $brat^{chs}$, whose function progressively declines with increasing temperature, therefore potentially decreasing the number of apoptotic cells in the brain. Collectively, these results confirm the ability of ZIKV to replicate and induce cell death in the adult $brat^{chs}$ brain, which could be relevant to human cancer and neurodegenerative diseases.

STAR★METHODS

Detailed methods are provided in the online version of this paper and include the following:

- KEY RESOURCES TABLE
- RESOURCE AVAILABILITY
  - Lead contact
  - Materials availability
  - Data and code availability
- EXPERIMENTAL MODEL AND SUBJECT DETAILS
  - *D. melanogaster* lines
  - Zika virus stocks
- METHOD DETAILS
  - Fly lifespan assessment
  - Fly infection method
  - Fly survival estimation
  - RNA isolation and quantitative real-time PCR
  - Immunostaining and antibodies
  - Climbing assays
- QUANTIFICATION AND STATISTICAL ANALYSIS

ACKNOWLEDGMENTS

We thank members of the Eleftherianos lab for maintaining and amplifying the laboratory fly lines and members of the Department of Biological Sciences at George Washington University for providing feedback to the project. Schematic figures were created using BioRender. The work was funded through a grant to I.E. from the Columbian College of Arts and Sciences at George Washington University. G.T.E. was funded through a Wilbur V. Harlan summer research fellowship from the George Washington University Department of Biological Sciences.

AUTHOR CONTRIBUTIONS

Conceptualization, G.T.E., S.C., and I.E.; methodology, G.T.E., D.B., S.C., and I.E.; investigation G.T.E., A.K., D.B., and S.C.; formal analysis G.T.E., D.B., S.C., and I.E; writing, G.T.E., S.C., and I.E.

DECLARATION OF INTERESTS

The authors declare no competing interests.

Received: September 19, 2022
Revised: December 18, 2022
Accepted: March 13, 2023
Published: March 16, 2023

REFERENCES

1. Musso, D., and Gubler, D.J. (2016). Zika virus. Clin. Microbiol. Rev. *29*, 487–524. https://doi.org/10.1128/CMR.00072-15.

2. Sharma, A., and Lal, S.K. (2017). Zika virus: transmission, detection, control, and prevention. Front. Microbiol. *8*, 110. https://doi.org/10.3389/fmicb.2017.00110.

3. Rothan, H.A., Fang, S., Mahesh, M., and Byrareddy, S.N. (2019). Zika virus and the metabolism of neuronal cells. Mol. Neurobiol. *56*, 2551–2557.

4. Bido-Medina, R., Wirsich, J., Rodríguez, M., Oviedo, J., Miches, I., Bido, P., Tusen, L., Stoeter, P., and Sadaghiani, S. (2018). Impact of Zika Virus on adult human brain structure and functional organization. Ann. Clin. Transl. Neurol. *5*, 752–762. https://doi.org/10.1002/acn3.575.

5. Coffey, L.L., Keesler, R.I., Pesavento, P.A., Woolard, K., Singapuri, A., Watanabe, J., Cruzen, C., Christe, K.L., Usachenko, J., Yee, J., et al. (2018). Intraamniotic Zika virus inoculation of pregnant rhesus macaques produces fetal neurologic disease. Nat. Commun. *9*, 2414.

6. Li, C., Xu, D., Ye, Q., Hong, S., Jiang, Y., Liu, X., Zhang, N., Shi, L., Qin, C.F., and Xu, Z. (2016). Zika virus disrupts neural progenitor development and leads to microcephaly in mice. Cell Stem Cell *19*, 120–126.

7. Adams Waldorf, K.M., Nelson, B.R., Stencel-Baerenwald, J.E., Studholme, C., Kapur, R.P., Armistead, B., Walker, C.L., Merillat, S., Vornhagen, J., Tisoncik-Go, J., et al. (2018). Congenital Zika virus infection as a silent pathology with loss of neurogenic output in the fetal brain. Nat. Med. *24*, 368–374.

8. Sasi, M.S., Rajendran, R., Meenakshy, V., Suresh, T., Heera Pillai, R., Dilip Kumar, T., Sugathan, A., and Regu, K. (2021). Study on vector dynamics of zika virus outbreak in thiruvananthapuram, Kerala, India. Int. J. Curr. Microbiol. App. Sci. *10*, 54–71. https://doi.org/10.20546/ijcmas.2021.1012.008.

9. Zhang, X., Li, G., Chen, G., Zhu, N., Wu, D., Wu, Y., and James, T.D. (2021). Recent progresses and remaining challenges for the detection of zika virus. Med. Res. Rev. *41*, 2039–2108. https://doi.org/10.1002/med.21786.

10. Lemaitre, B., Nicolas, E., Michaut, L., Reichhart, J.M., and Hoffmann, J.A. (1996). The dorsoventral regulatory gene cassette spätzle/Toll/cactus controls the potent antifungal response in *Drosophila* adults. Cell *86*, 973–983.

11. Liu, Y., Gordesky-Gold, B., Leney-Greene, M., Weinbren, N.L., Tudor, M., and Cherry, S. (2018). Inflammation-induced, STING-dependent autophagy restricts zika virus infection in the *Drosophila* brain. Cell Host Microbe *24*, 57–68.e3.

12. Goto, A., Okado, K., Martins, N., Cai, H., Barbier, V., Lamiable, O., Troxler, L., Santiago, E., Kuhn, L., Paik, D., et al. (2018). The kinase IKKβ regulates a STING- and NF-κB-Dependent antiviral response pathway in *Drosophila*. Immunity *49*, 225–234.e4. https://doi.org/10.1016/j.immuni.2018.07.013.

13. Martin, M., Hiroyasu, A., Guzman, R.M., Roberts, S.A., and Goodman, A.G. (2018). Analysis of *Drosophila* STING reveals an evolutionarily conserved antimicrobial function. Cell Rep. *23*, 3537–3550.e6. https://doi.org/10.1016/j.celrep.2018.05.029.

14. Tafesh-Edwards, G., and Eleftherianos, I. (2020). *Drosophila* immunity against natural and nonnatural viral pathogens. Virology *540*, 165–171.

15. Trammell, C.E., and Goodman, A.G. (2019). Emerging mechanisms of insulin-mediated antiviral immunity in *Drosophila melanogaster*. Front. Immunol. *10*, 2973. https://doi.org/10.3389/fimmu.2019.02973.

16. Hillyer, J.F. (2016). Insect immunology and hematopoiesis. Dev. Comp. Immunol. *58*, 102–118.

17. Buchon, N., Silverman, N., and Cherry, S. (2014). Immunity in *Drosophila melanogaster* — from microbial recognition to whole-organism physiology. Nat. Rev. Immunol. *14*, 796–810.

18. Hoffmann, J.A., and Reichhart, J.M. (2002). *Drosophila* innate immunity: an evolutionary perspective. Nature Immunol. *3*, 121–126.

19. Elrefaey, A.M.E., Hollinghurst, P., Reitmayer, C.M., Alphey, L., and Maringer, K. (2021). Innate immune antagonism of mosquito-borne flaviviruses in humans and mosquitoes. Viruses *13*, 2116. https://doi.org/10.3390/v13112116.

20. Mussabekova, A., Daeffler, L., and Imler, J.L. (2017). Innate and intrinsic antiviral immunity in *Drosophila*. Cell. Mol. Life Sci. *74*, 2039–2054.

21. Liu, Y., and Cherry, S. (2019). Zika virus infection activates sting-dependent antiviral autophagy in the *Drosophila* brain. Autophagy *15*, 174–175.

22. Delorme-Axford, E., and Klionsky, D.J. (2019). Inflammatory-dependent Sting activation induces antiviral autophagy to limit zika virus in the *Drosophila* brain. Autophagy *15*, 1–3.

23. Link, N., Chung, H., Jolly, A., Withers, M., Tepe, B., Arenkiel, B.R., Shah, P.S., Krogan, N.J., Aydin, H., Geckinli, B.B., et al. (2019). Mutations in ANKLE2, a ZIKA virus target, disrupt an asymmetric cell division pathway in *Drosophila* neuroblasts to cause microcephaly. Dev. Cell *51*, 713–729.e6.

24. Loewen, C., Boekhoff-Falk, G., Ganetzky, B., and Chtarbanova, S. (2018). A novel mutation in brain tumor causes both neural over-proliferation and neurodegeneration in adult *Drosophila*. G3 Genes *8*, 3331–3346.

25. Bello, B., Reichert, H., and Hirth, F. (2006). The brain tumor gene negatively regulates neural progenitor cell proliferation in the larval central brain of *Drosophila*. Development *133*, 2639–2648.

26. Betschinger, J., Mechtler, K., and Knoblich, J.A. (2006). Asymmetric segregation of the tumor suppressor brat regulates self-renewal in *Drosophila* neural stem cells. Cell *124*, 1241–1253.

27. Lee, C.Y., Wilkinson, B.D., Siegrist, S.E., Wharton, R.P., and Doe, C.Q. (2006). Brat is a Miranda cargo protein that promotes neuronal differentiation and inhibits neuroblast self-renewal. Dev. Cell *10*, 441–449.

28. Arama, E., Dickman, D., Kimchie, Z., Shearn, A., and Lev, Z. (2000). Mutations in the beta-propeller domain of the *Drosophila* brain tumor (brat) protein induce neoplasm in the larval brain. Oncogene *19*, 3706–3716. https://doi.org/10.1038/sj.onc.1203706.

29. Ferreira, P.G., Tesla, B., Horácio, E.C.A., Nahum, L.A., Brindley, M.A., de Oliveira Mendes, T.A., and Murdock, C.C. (2020). Temperature dramatically shapes mosquito gene expression with consequences for mosquito-zika virus interactions. Front. Microbiol. *11*, 901. https://doi.org/10.3389/fmicb.2020.00901.

30. Winokur, O.C., Main, B.J., Nicholson, J., and Barker, C.M. (2020). Impact of temperature on the extrinsic incubation period of Zika virus in *Aedes aegypti*. PLOS Negl. Trop. Dis. *14*, e0008047. https://doi.org/10.1371/journal.pntd.0008047.

31. Christofferson, R.C., and Mores, C.N. (2016). Potential for extrinsic incubation temperature to alter interplay between transmission potential and mortality of dengue-infected *Aedes aegypti*. Environ. Health Insights *10*, 119–123. https://doi.org/10.4137/EHI.S38345.

32. Villena, O.C., Ryan, S.J., Murdock, C.C., and Johnson, L.R. (2022). Temperature impacts the environmental suitability for malaria transmission by *Anopheles gambiae* and *Anopheles stephensi*. Ecology *103*, e3685. https://doi.org/10.1002/ecy.3685.

33. Tesla, B., Demakovsky, L.R., Mordecai, E.A., Ryan, S.J., Bonds, M.H., Ngonghala, C.N., Brindley, M.A., and Murdock, C.C. (2018). Temperature drives Zika virus transmission: evidence from empirical and mathematical models. Proc. Biol. Sci. *285*, 20180795. https://doi.org/10.1098/rspb.2018.0795.

34. Mordecai, E.A., Caldwell, J.M., Grossman, M.K., Lippi, C.A., Johnson, L.R., Neira, M., Rohr, J.R., Ryan, S.J., Savage, V., Shocket, M.S., et al. (2019). Thermal biology of mosquito-borne disease. Ecol. Lett. *22*, 1690–1708. https://doi.org/10.1111/ele.13335.

35. Murdock, C.C., Paaijmans, K.P., Cox-Foster, D., Read, A.F., and Thomas, M.B. (2012a). Rethinking vector immunology: the role of environmental temperature in shaping resistance. Nat. Rev. Microbiol. *10*, 869–876. https://doi.org/10.1038/nrmicro2900.

36. Murdock, C.C., Paaijmans, K.P., Bells, A.S., King, J.G., Hillyer, J.F., Read, A.F., and Thomas, M.B. (2012b). Complex effects of temperature on mosquito immune function.

Proc. R. Soc. B Biol. Sci. *279*, 3357–3366. https://doi.org/10.1098/rspb.2012.0638.

37. Balm, M.N.D., Lee, C.K., Lee, H.K., Chiu, L., Koay, E.S.C., and Tang, J.W. (2012). A diagnostic polymerase chain reaction assay for Zika virus. J. Med. Virol. *84*, 1501–1505. https://doi.org/10.1002/jmv.23241.

38. Elshahawi, H., Syed Hassan, S., and Balasubramaniam, V. (2019). Importance of zika virus NS5 protein for viral replication. Pathogens *8*, 169. https://doi.org/10.3390/pathogens8040169.

39. Thacker, S.A., Bonnette, P.C., and Duronio, R.J. (2003). The contribution of E2F-regulated transcription to *Drosophila PCNA* gene function. Curr. Biol. *13*, 53–58. https://doi.org/10.1016/s0960-9822(02)01400-8.

40. Jahn, T.R., Kohlhoff, K.J., Scott, M., Tartaglia, G.G., Lomas, D.A., Dobson, C.M., Vendruscolo, M., and Crowther, D.C. (2011). Detection of early locomotor abnormalities in a *Drosophila* model of Alzheimer's disease. J. Neurosci. Methods *197*, 186–189. https://doi.org/10.1016/j.jneumeth.2011.01.026.

41. Aggarwal, A., Reichert, H., and VijayRaghavan, K. (2019). A locomotor assay reveals deficits in heterozygous Parkinson's disease model and proprioceptive mutants in adult *Drosophila*. Proc. Natl. Acad. Sci. USA *116*, 24830–24839.

42. Carpenter, F.W. (1905). The reactions of the pomace fly (*Drosophila* ampelophila Loew) to light, gravity, and mechanical stimulation. Am. Nat. *39*, 157–171.

43. Greene, J.C., Whitworth, A.J., Kuo, I., Andrews, L.A., Feany, M.B., and Pallanck, L.J. (2003). Mitochondrial pathology and apoptotic muscle degeneration in *Drosophila* parkin mutants. Proc. Natl. Acad. Sci. USA *100*, 4078–4083.

44. Inagaki, H.K., Kamikouchi, A., and Ito, K. (2010). Methods for quantifying simple gravity sensing in *Drosophila melanogaster*. Nat. Protoc. *5*, 20–25.

45. Madabattula, S.T., Strautman, J.C., Bysice, A.M., O'Sullivan, J.A., Androschuk, A., Rosenfelt, C., Doucet, K., Rouleau, G., and Bolduc, F. (2015). Quantitative analysis of climbing defects in a *Drosophila* model of neurodegenerative disorders. J. Vis. Exp. *100*, e52741.

46. Saleh, M.C., Tassetto, M., van Rij, R.P., Goic, B., Gausson, V., Berry, B., Jacquier, C., Antoniewski, C., and Andino, R. (2009). Antiviral immunity in *Drosophila* requires systemic RNA interference spread. Nature *458*, 346–350. https://doi.org/10.1038/nature07712.

47. Swevers, L., Liu, J., and Smagghe, G. (2018). Defense mechanisms against viral infection in *Drosophila*: RNAi and non-RNAi. Viruses *10*, 230.

48. Heigwer, F., Port, F., and Boutros, M. (2018). RNA interference (RNAi) screening in *Drosophila*. Genetics *208*, 853–874. https://doi.org/10.1534/genetics.117.300077.

49. Blázquez, A.B., and Saiz, J.C. (2016). Neurological manifestations of Zika virus infection. World J. Virol. *5*, 135–143. https://doi.org/10.5501/wjv.v5.i4.135.

50. Araujo, A.Q.C., Silva, M.T.T., and Araujo, A.P. (2016). Zika virus-associated neurological disorders: a review. Brain. *139*, 2122–2130. https://doi.org/10.1093/brain/aww158.

51. Acosta-Ampudia, Y., Monsalve, D.M., Castillo-Medina, L.F., Rodríguez, Y., Pacheco, Y., Halstead, S., Willison, H.J., Anaya, J.M., and Ramírez-Santana, C. (2018). Autoimmune neurological conditions associated with zika virus infection. Front. Mol. Neurosci. *11*, 116. https://doi.org/10.3389/fnmol.2018.00116.

52. Charniga, K., Cucunubá, Z.M., Walteros, D.M., Mercado, M., Prieto, F., Ospina, M., Nouvellet, P., and Donnelly, C.A. (2021). Descriptive analysis of surveillance data for Zika virus disease and Zika virus-associated neurological complications in Colombia, 2015-2017. PLoS One *16*, e0252236. https://doi.org/10.1371/journal.pone.0252236.

53. Mehrbod, P., Ande, S.R., Alizadeh, J., Rahimizadeh, S., Shariati, A., Malek, H., Hashemi, M., Glover, K.K.M., Sher, A.A., Coombs, K.M., and Ghavami, S. (2019). The roles of apoptosis, autophagy and unfolded protein response in arbovirus, influenza virus, and HIV infections. Virulence *10*, 376–413. https://doi.org/10.1080/21505594.2019.1605803.

54. Lee, J.K., Kim, J.A., Oh, S.J., Lee, E.W., and Shin, O.S. (2020). Zika virus induces tumor necrosis factor-related apoptosis inducing ligand (TRAIL)-Mediated apoptosis in human neural progenitor cells. Cells *9*, 2487. https://doi.org/10.3390/cells9112487.

55. Ferraris, P., Cochet, M., Hamel, R., Gladwyn-Ng, I., Alfano, C., Diop, F., Garcia, D., Talignani, L., Montero-Menei, C.N., Nougairede, A., et al. (2019). Zika virus differentially infects human neural progenitor cells according to their state of differentiation and dysregulates neurogenesis through the Notch pathway. Emerg. Microbes Infect. *8*, 1003–1016.

56. Liu, C., Shan, Z., Diao, J., Wen, W., and Wang, W. (2019). Crystal structure of the coiled-coil domain of *Drosophila* TRIM protein Brat. Proteins *87*, 706–710. https://doi.org/10.1002/prot.25691.

57. Belmonte, R.L., Corbally, M.K., Duneau, D.F., and Regan, J.C. (2019). Sexual dimorphisms in innate immunity and responses to infection in *Drosophila melanogaster*. Front. Immunol. *10*, 3075. https://doi.org/10.3389/fimmu.2019.03075.

58. Vincent, C.M., and Sharp, N.P. (2014). Sexual antagonism for resistance and tolerance to infection in *Drosophila melanogaster*. Proc. R. Soc. B. Biol. Sci. *281*, 20140987. https://doi.org/10.1098/rspb.2014.0987.

59. Palmer, W.H., Medd, N.C., Beard, P.M., and Obbard, D.J. (2018). Isolation of a natural DNA virus of *Drosophila melanogaster*, and characterisation of host resistance and immune responses. PLoS Pathog. *14*, e1007050. https://doi.org/10.1371/journal.ppat.1007050.

60. Klein, S.L., and Flanagan, K.L. (2016). Sex differences in immune responses. Nat. Rev. Immunol. *16*, 626–638. https://doi.org/10.1038/nri.2016.90.

61. Tafesh-Edwards, G., Kalukin, A., and Eleftherianos, I. (2022). Zika virus induces sex-dependent metabolic changes in *Drosophila melanogaster* to promote viral replication. Front. Immunol. *13*, 903860. https://doi.org/10.3389/fimmu.2022.903860.

62. Harsh, S., Ozakman, Y., Kitchen, S.M., Paquin-Proulx, D., Nixon, D.F., and Eleftherianos, I. (2018). Dicer-2 regulates resistance and maintains homeostasis against zika virus infection in *Drosophila*. J. Immunol. *201*, 3058–3072.

63. Wang, Z., Wu, D., Liu, Y., Xia, X., Gong, W., Qiu, Y., Yang, J., Zheng, Y., Li, J., Wang, Y.F., et al. (2015). *Drosophila* Dicer-2 has an RNA interference-independent function that modulates Toll immune signaling. Sci. Adv. *1*, e1500228. https://doi.org/10.1126/sciadv.1500228.

64. Deddouche, S., Matt, N., Budd, A., Mueller, S., Kemp, C., Galiana-Arnoux, D., Dostert, C., Antoniewski, C., Hoffmann, J.A., and Imler, J.L. (2008). The DExD/H-box helicase Dicer-2 mediates the induction of antiviral activity in *Drosophila*. Nat. Immunol. *9*, 1425–1432. https://doi.org/10.1038/ni.1664.

65. Schindelin, J., Arganda-Carreras, I., Frise, E., Kaynig, V., Longair, M., Pietzsch, T., Preibisch, S., Rueden, C., Saalfeld, S., Schmid, B., et al. (2012). Fiji: an open-source platform for biological-image analysis. Nat. Methods *9*, 676–682. https://doi.org/10.1038/nmeth.2019.

66. Park, J., Lee, S.B., Lee, S., Kim, Y., Song, S., Kim, S., Bae, E., Kim, J., Shong, M., Kim, J.M., and Chung, J. (2006). Mitochondrial dysfunction in *Drosophila* PINK1 mutants is complemented by parkin. Nature *441*, 1157–1161.

67. Livak, K.J., and Schmittgen, T.D. (2001). Analysis of relative gene expression data using realtime quantitative PCR, and the 2–11ct method. Methods *25*, 402–408.

68. Schmittgen, T.D., and Livak, K.J. (2008). Analyzing real-time PCR data by the comparative CT method. Nat. Protoc. *3*, 1101–1108. https://doi.org/10.1038/nprot.2008.73.

STAR★METHODS

KEY RESOURCES TABLE

REAGENT or RESOURCE	SOURCE	IDENTIFIER
Antibodies		
rabbit anti-Flavivirus (clone: D1-4G2-4-15 (4G2))	Enzo Life Sciences	ABS491-0200
chicken anti-GFP	Invitrogen™	A10262
mouse anti-Repo	DSHB	8D12 (contributed by C. Goodman, University of California-Berkley)
rat anti-elav	DSHB	7E8A10 (contributed by G.E. Rubin, Janelia Farm)
goat anti-rabbit AlexaFluor® 568	Invitrogen™	A11011
goat anti-chicken AlexaFluor® 488	Invitrogen™	A11039
goat anti-mouse AlexaFluor® 647	Invitrogen™	A21242
goat anti-rat AlexaFluor® 633	Invitrogen™	A21094
Bacterial and virus strains		
MR766	Harsh et al., 2018[62]	N/A
Chemicals, peptides, and recombinant proteins		
Phosphate buffered saline (PBS)	Quality Biological	119-069-131
Phosphate buffered saline (PBS)	VWR	97062–948
TRIzol Reagent	Invitrogen	Cat# 15596026
Triton X-100 (SURFACT-AMPS X-100)	Thermo Scientific™	28314
Prolong Diamond Antifade Mountant with DAPI	Molecular Probes™	P36962
16% Paraformaldehyde Aqueous Solution, EM Grade	Electron Microscopy Sciences	15710-S
Normal Goat Serum	MP Biomedicals™	ICN19135680
Experimental models: Organisms/strains		
Fruit fly: *brat^{chs}/Cyo; pcna-GFP/Tm3,ser*	Loewen et al.,[24]	N/A
Fruit fly: *pcna-GFP*	Loewen et al.,[24]	N/A
Oligonucleotides		
Primer: ZikaNS5 Forward: CCTTGGATTCTTGAACGAGGA	Harsh et al.[62]	N/A
Primer: ZikaNS5 Reverse: AGAGCTTCATTCTCCAGATCAA	Harsh et al.[62]	N/A
Primer: RpL32 Forward: GATGACCATCCGCCCAGCA	Harsh et al.[62]	N/A
Primer: RpL32 Reverse: CGGACCGACAGCTGCTTGGC	Harsh et al.[62]	N/A
Primer: Dicer-2 Forward: GTATGGCGATAGTGTGACTGCGAC	Harsh et al.[62]	N/A
Primer: Dicer-2 Reverse: GCAGCTTGTTCCGCAGCAATATAGC	Harsh et al.[62]	N/A
Primer: Argonaute-2 Forward: CCGGAAGTGACTGTGACAGATCG	Harsh et al.[62]	N/A
Primer: Argonaute-2 Reverse: CCTCCACGCACTGCATTGCTCG	Harsh et al.[62]	N/A
Primer: Reaper Forward: CATACCCGATCAGGCGACTC	This study	N/A

(*Continued on next page*)

Continued

REAGENT or RESOURCE	SOURCE	IDENTIFIER
Primer: Reaper Reverse: ACATGAAGTGTACTGGCGCA	This study	N/A
Primer: Hid Forward: ACTGCAATTTCAATGTCTTCGCA	This study	N/A
Primer: Hid Reverse: AGATGTGCTTGTTTTTGTGGACT	This study	N/A
Primer: Grim Forward: CAATATTTCCGTGCCGCTGG	This study	N/A
Primer: Grim Reverse: ATCCCAGCATCCAAACTCCG	This study	N/A
Software and algorithms		
PRISM	GraphPad Software	Version 9
Fiji	Schindelin et al.,[65]	Version: 2.3.0/1.53q
Other		
Bloomington *Drosophila* food	LabExpress	Cat# 7001-NV
Baker's yeast	Carolina Biological Supply	Cat# 173235
Nanoject III	Drummond Scientific	Cat# 3-000-207
Nanoject II	Drummond Scientific	Cat# 3-000-204
Nutri-Fly® Bloomington Formulation *Drosophila* food	Genesee Scientific	Cat# 66-113
Nikon Eclipse Ti2 confocal microscope	Nikon	N/A

RESOURCE AVAILABILITY

Lead contact

Further information and requests for resources and reagents should be directed to Dr. Ioannis Eleftherianos (ioannise@gwu.edu).

Materials availability

The *brat^{chs}/Cyo; pcna-GFP/Tm3,ser* and *pcna-GFP* strains are available to other laboratories upon request to the lead contact.

Data and code availability

- All data reported in this paper will be shared by the lead contact upon request.
- This paper does not report original code.

EXPERIMENTAL MODEL AND SUBJECT DETAILS

D. melanogaster lines

All fly stocks used in this study are *Wolbachia*-free and listed in key resources table. Flies were reared on Bloomington *Drosophila* Stock Center cornmeal food (LabExpress), supplemented with yeast (Carolina Biological Supply), and maintained at 25°C with a 12:12-h light:dark photoperiodic cycle. Flies used in the immunostaining experiments were reared on a Nutri-Fly Bloomington Formulation food (Genesee Scientific) and maintained at 25°C with a 12:12-h light:dark photoperiodic cycle. Homozygous female and male *brat^{chs}* flies (5–7-day-old) carrying both the *brat^{chs}* mutation and a reporter gene (*pcna-GFP*) were used for experiments. The *pcna-GFP* stock was used as a genetic background control. Both sexes were selected from the same generation and randomly assigned to experimental groups.

Zika virus stocks

Stocks of ZIKV strain MR766 were prepared as previously described.[62]

METHOD DETAILS

Fly lifespan assessment

For lifespan assessment, newly eclosed flies were collected under light carbon dioxide (CO_2) anesthesia and housed at a density of 15–20 females and 15–20 males each per vial. At least 100 males and 100 females were tested for each fly line. Flies were kept on Bloomington *Drosophila* Stock Center cornmeal food (LabExpress), supplemented with yeast (Carolina Biological Supply), and maintained at 25°C or 29°C with a 12:12-h light:dark cycle. They were transferred to fresh vials every third day for the duration of the experiment, and mortality was recorded daily.

Fly infection method

Injections were performed by anesthetizing flies of the stated genotypes with CO_2. For each experiment, female and male flies were injected with ZIKV suspensions in PBS (pH 7.5) using a nanoinjector (Nanoject II for immunostaining experiments and Nanoject III for all other experiments; Drummond Scientific). ZIKV stocks were prepared in PBS (pH 7.5). Live ZIKV solution (11,000 PFU/fly) (100 nL) were injected into the thorax of flies, and control flies were injected with the same volume of PBS. Following infection, flies were maintained at 25°C or 29°C and transferred to fresh vials every third day for the duration of the experiment. Flies were collected at 4 days post injection and directly processed for RNA analysis. Fly deaths occurring within one day of injection were attributed to injury and were not included in the results.

Fly survival estimation

For each fly strain, three groups of 20 male and female flies were injected with ZIKV, and control groups were injected with PBS. Following injection, flies were maintained at a constant temperature of 25°C or 29°C with a 12-h light/dark cycle, and mortality was recorded daily.

RNA isolation and quantitative real-time PCR

For each experiment, total RNA was extracted from 10 male or female flies, using TRIzol (Invitrogen) according to manufacturer's protocol. Total RNA (500 ng–1 μg) was used to synthesize cDNA using the High-Capacity cDNA Reverse Transcription Kit (Applied Biosystems). Quantitative RT-PCR (qRT-PCR) experiments were performed with two technical replicates and gene-specific primers (key resources table) using a CFX96 Real-Time PCR detection system (Bio-Rad Laboratories). Cycle conditions were as follows: 95°C for 2 min, 40 repetitions of 95°C for 15 s followed by 61°C for 30 s, and then one round of 95°C for 15 s, 65°C for 5 s, and finally 95°C for 5 s.

Immunostaining and antibodies

Flies of each genotype and sex were collected at 0–2 days after eclosion and aged to 5–7 days old. Then, ZIKV infection was administered via the injection procedure described previously. After injection, flies were maintained at 29°C. Brains were dissected in PBS1X from surviving flies at 4 days post injection and transferred into fixative solution. Brains were fixed for 30 min in 4% paraformaldehyde (4% PFA) in PBS1X and placed on a rotating shaker. The fixative solution was removed, and the brains were then washed with PBS-Triton X-100 0.1–0.3% (PBS-T). This included three wash steps of 30 min at room temperature on a shaker, removing the PBS-T at each step, and replacing with fresh PBS-T. After the final wash, brains were placed in a blocking solution of PBS-T and 4% Normal Goat Serum for 1 h at room temperature. Once blocking solution was removed, primary antibodies were added and incubated overnight at 4°C. The primary antibodies' dilutions used were as follows: rabbit-*anti*-Flavivirus (4G2) 1:100, chicken-*anti*-GFP 1:500, rat-*anti*-Elav 1:100, mouse-*anti*-Repo 1:50. After removing the primary antibodies, three additional wash steps were performed with PBS-T on a rotating shaker for 30 min. Secondary antibodies were then added with brains and incubated at room temperature for 3 h on a rotating shaker. The secondary antibodies' dilutions used were as follows: goat anti-rabbit AlexaFluor 568 1:1000, goat anti-chicken AlexaFluor 488 1:1000, goat anti-rat AlexaFluor 633 1:1000, goat anti-mouse AlexaFluor 647 1:1000. Next, the secondary antibodies were removed, and brains were washed with PBS-T for 15 min three times on a rotating shaker. Finally, brains were transferred into a drop of Prolong Diamond Antifade Mountant with DAPI on a microscope slide. Images were acquired with Nikon Eclipse Ti2 Laser Scanning Confocal Microscope and processed using Fiji ImageJ2 (Version: 2.3.0/1.53q). Image acquisition was done using the same camera settings between genotypes and treatments. Immunofluorescence images represent stacks of images that were generated using the Standard Deviation z stack function in Fiji ImageJ2. 'Brightness and contrast' function in Fiji ImageJ2 was used to improve visualization; however, all measurements

and quantification were done on unmanipulated files. Quantification of flavivirus antigen immunofluorescence was done using the 'Analyze particles' function in Fiji ImageJ2. Briefly, a 'Maximum projection' function was applied to 68 Z-stacks for all experimental samples in the Grayscale mode. For each resulting image, a region of interest (ROI) was selected based on DAPI staining. The image threshold for all samples was similarly adjusted, and the 'Analyze particles' function used to determine the % immunostained area compared to the total imaged brain area based on the selected ROI. Fluorescence intensity plots for all immunostainings (4G2, Repo or Elav, GFP and DAPI) were obtained as previously described[62] using a single image chosen from the corresponding z-stacks. Measurements were done using the same ROI across all four fluorescence channels and across experimental groups.

Climbing assays

Climbing assays were carried out as previously described.[45,66] Groups of 10 adult female and male flies were transferred into empty vials and incubated for 1 h at room temperature for acclimatization. The flies were gently tapped down to the bottom of the vials and then the number of flies reaching an 8 cm mark was counted after 18 s of climbing.

QUANTIFICATION AND STATISTICAL ANALYSIS

All analyses were conducted with data from three independent experiments. For survival curves, pairwise comparisons of each experimental group with its control were carried out using a log-rank (Mantel–Cox) test. For climbing experiments, a Student *t* test was used to measure the statistical significance (Scale bar, 100 mm *p < 0.05, **p < 0.05, ****p < 0.0001). Data from quantitative real-time PCR was analyzed with gene specific primers in duplicates, with at least three independent experiments for both test and control treatments. Fold changes were calculated with the $2^{-\Delta\Delta C}{}_{T}$ method using *Ribosomal protein L32* (*RpL32*), also known as *rp49*, as a housekeeping gene.[67,68] All error bars represent standard error of mean. GraphPad Prism software was used for statistical analysis.